Biochimica et Biophysica Acta 1837 (2014) 1219–1225

Contents lists available at ScienceDirect

Biochimica et Biophysica Acta

journal homepage: www.elsevier.com/locate/bbabio

Probing the ubiquinol-binding site of recombinant *Sauromatum guttatum* alternative oxidase expressed in *E. coli* membranes through site-directed mutagenesis☆

Luke Young [a], Benjamin May [a], Alice Pendlebury-Watt [a], Julia Shearman [a], Catherine Elliott [a], Mary S. Albury [a], Tomoo Shiba [b], Daniel Ken Inaoka [c], Shigeharu Harada [b], Kiyoshi Kita [c], Anthony L. Moore [a,*]

[a] Biochemistry and Molecular Sciences, School of Life Sciences, University of Sussex, Falmer, Brighton BN1 9QG, UK
[b] Department of Applied Biology, Graduate School of Science and Technology, Kyoto Institute of Technology, Kyoto 606-8585, Japan
[c] Department of Biomedical Chemistry, Graduate School of Medicine, The University of Tokyo, Tokyo 113-0033, Japan

ARTICLE INFO

Article history:
Received 9 December 2013
Received in revised form 23 January 2014
Accepted 28 January 2014
Available online 12 February 2014

Keywords:
Alternative oxidase
Quinol oxidase
Oxygen affinity
Structure–function relation
Site-directed mutagenesis
Escherichia coli membrane
AOX inhibitors

ABSTRACT

In the present paper we have investigated the effect of mutagenesis of a number of highly conserved residues (R159, D163, L177 and L267) which we have recently shown to line the hydrophobic inhibitor/substrate cavity in the alternative oxidases (AOXs). Measurements of respiratory activity in rSgAOX expressed in *Escherichia coli* FN102 membranes indicate that all mutants result in a decrease in maximum activity of AOX and in some cases (D163 and L177) a decrease in the apparent K_m (O_2). Of particular importance was the finding that when the L177 and L267 residues, which appear to cause a bottleneck in the hydrophobic cavity, are mutated to alanine the sensitivity to AOX antagonists is reduced. When non-AOX anti-malarial inhibitors were also tested against these mutants widening the bottleneck through removal of isobutyl side chain allowed access of these bulkier inhibitors to the active-site and resulted in inhibition. Results are discussed in terms of how these mutations have altered the way in which the AOX's catalytic cycle is controlled and since maximum activity is decreased we predict that such mutations result in an increase in the steady state level of at least one O_2-derived AOX intermediate. Such mutations should therefore prove to be useful in future stopped-flow and electron paramagnetic resonance experiments in attempts to understand the catalytic cycle of the alternative oxidase which may prove to be important in future rational drug design to treat diseases such as trypanosomiasis. Furthermore since single amino acid mutations in inhibitor/substrate pockets have been found to be the cause of multi-drug resistant strains of malaria, the decrease in sensitivity to main AOX antagonists observed in the L-mutants studied in this report suggests that an emergence of drug resistance to trypanosomiasis may also be possible. Therefore we suggest that the design of future AOX inhibitors should have structures that are less reliant on the orientation by the two-leucine residues. This article is part of a Special Issue entitled: 18th European Bioenergetic Conference.

1. Introduction

The alternative oxidase is a ubiquinol oxidoreductase that catalyses the four electron reduction of oxygen to water. It is now generally recognized that the distribution of the alternative oxidase is substantially wider than previously thought [1]. It is ubiquitous amongst plants, and also found in some agrochemically important fungi (such as *Septoria tritici* — a wheat pathogen) and protists [1,2]. Importantly it is also widespread amongst human parasites such as *Trypanosoma brucei* (the causative agent of African Sleeping Sickness) [3,4], intestinal parasites such as *Cryptosporidium parvum* [5,6] and *Blastocystis hominis* [7] and opportunistic human pathogens such as *Candida albicans* [8]. It should be noted that immunocompromised individuals are particularly susceptible to these opportunistic human diseases, and new drugs that are well tolerated and have clearly defined biochemical targets are therefore urgently required [9]. Since the alternative oxidase is absent from the human host and is essential for the life-cycle of the trypanosomal parasite within the blood-stream [4] there is growing support for this protein to be considered as a viable target for the treatment of trypanosomiasis and indeed other diseases in which the alternative oxidase plays a key metabolic role [10–12]. Indeed treatment of mice infected with trypanosomes by the antibiotic ascofuranone at sub-nM concentrations rapidly clears the parasite from the blood-stream without any adverse effects upon the animal [13]. Furthermore the chemotherapeutic efficacy of ascofuranone *in vivo* has also been confirmed [14].

Abbreviations: Q(H_2), (reduced) ubiquinone; OG, octyl gallate; SHAM, salicylic hydroxamic acid; CB, colletochlorin B; Asco, ascofuranone; AOX, alternative oxidase; rSgAOX, recombinant *Sauromatum guttatum* alternative oxidase

☆ This article is part of a Special Issue entitled: 18th European Bioenergetic Conference.

* Corresponding author. Tel.: +44 1273 678479; fax: +44 1273 678433.
E-mail address: a.l.moore@sussex.ac.uk (A.L. Moore).

http://dx.doi.org/10.1016/j.bbabio.2014.01.027
0005-2728/

Prior to the recent structural elucidation of the trypanosomal AOX [15], generally accepted structural models predicted that the AOX is an integral interfacial monotopic protein that interacts with a single leaflet of the lipid bilayer and contains a non-haem diiron carboxylate active site [1,16,17]. Such models are supported by extensive site-directed mutagenesis and spectroscopic studies [18–25]. Non-haem diiron-containing enzymes are a ubiquitous and diverse super-family of metalloenzymes [26]. They can be divided into different sub-families with a wide range of distinct catalytic functions such as oxidation, hydroxylation or desaturation and act on a wide variety of substrates. Despite their different activities, many of the enzymes in this family share very common structural elements. These include a common fold involving a four-helix bundle, a bridging carboxylate group in the diiron site and the presence of common ligands [26]. In addition they all possess a common catalytic function namely the activation of molecular oxygen [9,10]. The alternative oxidases are the newest and currently largest sub-class of the diiron protein family. The acquisition of a high-resolution structure of the alternative oxidase is a major breakthrough since it not only represents the first structure of any AOX or a membrane-bound diiron protein but also is the last of the mitochondrial respiratory quinol oxidases to be solved [15]. Crystal structures confirmed that the AOX is a homo-dimer with each monomer being comprised of 6 long α-helices, 4 of which form a 4 helix bundle which acts as a scaffold to bind the two iron atoms (connected by hydroxo bridge). The iron atoms within the active-site under oxidised conditions are co-ordinated by 4 glutamate residues but no histidine residues which is an unusual co-ordination for a diiron protein [15,26]. Of particular significance was the finding that the redox-active tyrosine (Y275 — *Sauromatum guttatum* numbering) is within 4 Å of the active-site consistent with its proposed role in the oxygen reduction cycle [1,27]. In addition to the wild-type enzyme, high-resolution structures of the active site of the protein in the presence of ascofuranone-derivatives, AF2779OH and colletochlorin B have also been described [15]. Such structures revealed the presence of a hydrophobic channel that connects the diiron centre with the interior of the lipid bilayer in a manner analogous to the channels observed in the yeast NADH dehydrogenase (Ndi1) [28], prostaglandin H_2 synthase [29] and Complex I [30]. All of the inhibitors appeared to enter the AOX active-site *via* this hydrophobic channel and docking studies suggest that it is also the channel through which ubiquinol enters and binds to the active-site [15,27].

In an attempt to further probe the nature of the substrate-binding site, we have generated a number of mutants within the diiron centre and at the entrance to the hydrophobic pocket in rSgAOX. Mutagenesis of highly conserved residues (R159, D163, L177 and L267) to alanine, all of which line the hydrophobic inhibitor/substrate cavity in AOX, resulted in a decrease in maximum activity of AOX and in the case of D163 and L177 a decrease in the apparent K_m (O_2). Of particular interest was the finding that the mutation of both L177 and L267 severely reduced the sensitivity of rSgAOX to AOX antagonists colletochlorin B and ascofuranone whilst increasing the sensitivity to bulky quinolone antimalarials. Such results are consistent with these residues acting as a gate to orientate substrates and inhibitors into the correct conformation to enter the active-site.

2. Materials and methods

2.1. Strains

The *Escherichia coli* strains DH5α and JM110 were used for amplification of plasmids and FN102 [31] for expression of rSgAOX.

2.2. Site-directed mutagenesis and plasmid construction

The *S. guttatum* AOX lacking the mitochondrial targeting signal sequence was used for expression in *E. coli*. Prediction of the cleavage site was performed using MitoProt (http://ihg2.helmholtz-muenchen.de/ihg/mitoprot.html) [32]. In order to remove the leader sequence and facilitate cloning, a recognition site for *Nde*I was introduced at the cleavage site of the AOX. Firstly the orientation of the AOX cDNA in pAOSG81 [33] was reversed by digestion with *Eco*RI followed by ligation of the resulting fragments to give pAOSG/R. This plasmid, together with primers 5′-GTTCTCGCCCCCCCGCCATATGAGCACGCTGTCAGC-3′ and 5′-GCTGACAGCGTGCTCATATGGCGGGGGGGCGAGAAC-3′ was used to incorporate the *Nde*I site (alteration underlined) and was performed using the Quick-Change mutagenesis kit (Stratagene) according to the manufacturer's instructions. The mature AOX sequence was removed on an *Nde*I–*Bam*HI fragment and ligated to *Nde*I–*Bam*HI digested pET15b (Novagen) to produce the expression construct pET.SgAOX. The recognition sequence of the *Nco*I site present in the pET vector was removed, by altering to GCATGG, in order to facilitate the construction of AOX mutants.

Construction of pET.T179A was carried out by removal of an *Nco*I–*Bam*HI fragment from pREP1-T179A [34] and ligation to *Nco*I–*Bam*HI digested pET.SgAOX.

Mutagenesis of AOX was performed using the Quick Change mutagenesis kit (Stratagene) according to the manufacturer's instructions. The list in Section 2.3 describes the oligonucleotides used for each mutation, with altered codons in bold and underlined. Mutagenesis was carried out with pSLM-AOR [21] yielding pQC.L177A, pQC.L267A, pQC.R159A and pQC.D163A respectively.

pQC.L177A and pQC.L267A were used initially to construct plasmids for expression in *Schizosaccharomyces pombe*. Each full-length mutant AOX was excised on a *Bsp*HI–*Bam*HI fragment and ligated to the yeast expression vector pREP1/N (a modified version of pREP1 [35] in which the *Nde*I site was replaced with *Nco*I), which had been digested with *Nco*I and *Bam*HI, yielding pREP1-L177A and pREP1-L267A. For *E. coli* expression, the mutant AOX fragment was removed from the yeast vector on an *Nco*I–*Bam*HI fragment and ligated to *Nco*I–*Bam*HI digested pET.SgAOX to produce pET.L177A and pET.L267A, respectively. Construction of pET.R159A and pET.D163A was carried out by removal of the mutant AOX on an *Nco*I–*Bam*HI fragment from pQC.R159A and pQC.D163A. The mutant AOX fragments were ligated to *Nco*I–*Bam*HI digested pET.SgAOX to produce pET.R159A and pET.D163A, respectively.

2.3. Primers

Oligonucleotides used for site-directed mutagenesis to produce mutated forms of *S. guttatum* AOX. Altered codons are in bold and underlined.

Mutation	Primer sequence	
L177A	L177A/F	CGG GCG ATG ATG **GCG** GAG ACG GTG GC
	L177A/R	GC CAC CGT CTC **CGC** CAT CAT CGC CCG
L267A	L267A/F	GTT GTG GGC TAC **GCG** GAG GAG GAG GCC
	L267A/F	GGC CTC CTC CTC **CGC** GTA GCC CAC AAC
R159A	R159A/F	C GTC AAG GCC CTC **GCG** TGG CCC ACC GAC
	R159A/R	GTC GGT GGG CCA **CGC** GAG GGC CTT GAC G
D163A	D163A/F	CGG TGG CCC ACC **GCG** ATC TTC TTC CAG C
	D163A/R	G CTG GAA GAA GAT **CGC** GGT GGG CCA CCG

2.4. Expression of rSgAOX in E. coli membranes

E. coli (FN102) cells were transformed with the pET.SgAOX construct, and grown overnight on selective Luria agar supplemented with 100 μg/ml amino-levulinic acid (ALA), 50 μg/ml kanamycin and 100 μg/ml ampicillin. A single colony was used to streak a fresh agar plate with the same supplements, and was incubated for 12 h at 37 °C. A scrape of cells from the streak plate was used to inoculate 50 ml starter culture (Luria broth, 100 μg/ml ALA, 50 μg/ml kanamycin, 50 μg/ml ampicillin). The starter culture was grown at 37 °C with shaking for ~4 h, followed by centrifugation at 8000 *g* for 5 min and resuspension

in 5 ml of non-supplemented Luria broth in order to remove the ALA from the media. The centrifugation and resuspension step was repeated, and the resultant cell suspension was used to inoculate 5 l of K-broth (50 g tryptone–peptone, 25 g yeast extract, 25 g casamino acid, 52 g dipotassium hydrogen orthophosphate, 15 g potassium dihydrogen orthophosphate, 3.7 g trisodium citrate, 12.5 g ammonium sulphate, 0.25 g magnesium sulphate, 0.125 g iron sulphate, 0.125 g iron chloride, 100 g glucose and 0.5 g carbenicillin). The cultures were incubated with shaking at 30 °C until the $OD_{600} = 0.1$, at which point the cells were induced with 25 μM IPTG. After induction, the cultures were incubated for a further 14 h at 30 °C with shaking.

Following the 14-hour growth period, cells were harvested by centrifugation at 8000 *g* (10 min) and cell pellets were resuspended in 50 mM Tris–HCl, 10 mM pyruvate, pH 7.5. After the pellets were pooled and homogenised, a protease inhibitor cocktail (Roche "Complete") was added, before lysis using a French Press (10 k psi, two passes). After lysis, cell debris was removed in a single 12,000 *g* centrifugation step (15 min), and the supernatant was centrifuged for 1 h at 200,000 *g*. The pellets containing membrane were then resuspended in a minimal volume of 50 mM Tris–HCl, 10 mM pyruvate, pH 7.5 prior to snap freezing, storage or experimentation.

2.5. Oxygen uptake

Respiratory activity was measured with a Clark-type electrode (Rank Brothers, Cambridge, U.K.) using 0.1–0.5 mg *E. coli* membranes suspended in 0.4 ml air-saturated reaction medium (250 μM at 25 °C) containing 50 mM Tris–HCl (pH 7.5).

2.6. Oxygen affinity

O_2 levels were recorded continuously, in the presence of antimycin A and KCN, until anaerobiosis occurred. The derivative with respect to time of these O_2 traces was calculated with Chart software (ADInstruments) using a window of 16.5 s (11 data points), which allowed expression of O_2 uptake rates as a function of the corresponding O_2 levels. Estimations of AOX's affinity for O_2 from respiratory traces are subject to potential pitfalls, as respiratory activity is not necessarily controlled exclusively by AOX activity, but also by that of substrate dehydrogenases [36]. We have shown previously, however, that AOX exerts nearly 95% of total flux control over inhibitor resistant NADH oxidation in isolated *S. pombe* mitochondria [36] and the results presented in Table S1 suggest that this is also the case with *E. coli* membrane bound AOX. For instance wild-type and mutant NDH-2 activity considerably exceeds the maximal AOX activity (Table S1). Hence when respiration is limited by oxygen, this will therefore be the direct result of the kinetic characteristics of AOX [34]. Table S1 also demonstrates that none of the AOX inhibitors tested in this publication had any effect upon either wild-type or mutated AOX NDH-2 activity.

2.7. Colletochlorin B synthesis

Colletochlorin B was synthesised using the technique described by [37], with minor modifications to the final product purification. The product was purified *via* flash chromatography (petrol ether 40–80: diethyl ether 10:1 → 4:1), followed by recrystallisation from chloroform to obtain the compound as white needles in 20% yield.

2.8. General molecular biology procedures

Oligonucleotides were obtained from MWG Biotech. Sequencing was performed by Beckman Coulter Genomics. Other procedures were as described by Sambrook et al. [38].

All chemicals were of biochemistry grade. The protease inhibitor 'cocktail' was purchased from Roche.

3. Results

We previously ascertained the location of the ubiquinol-binding site by soaking TAO crystals with specific AOX inhibitors such as ascofuranone derivatives (AF27709OH) and colletochlorin B (CB) [15]. X-ray data indicated that the two inhibitors bind in a very similar manner approximately 4–5 Å from the diiron centre and CAVER visualisation software [39] revealed that both are located within a hydrophobic cavity which stretches from the diiron centre to the interior of the phospholipid bilayer. We refer to this channel as the L-channel owing to the presence of two leucine residues located at the centre of the channel. The L-cavity is located (Fig. 1A) between the membrane-binding helices α-1 and α-4 and is mostly lined by highly conserved hydrophobic and charged residues (V155, R159, R173, L177, V180, L267, E270, A271 and S/T274 — note SgAOX numbering used throughout) some of which we have previously shown to be essential for catalytic activity [1,15,18]. An important aspect of the channel is that although it is ~18–20 Å long from the surface of the protein to the diiron centre at the cavity entrance, which is framed by helices α1 and α4, it is approximately 12 Å wide. It then narrows to a width of approximately 6.5 Å at the location of L177 and L267 before widening at the entrance to the active-site (Fig. 1B). We have previously built a ubiquinone-binding model by superimposing a ubiquinol molecule onto the bound structure of the TAO–AF27709OH complex [15] and similar models have been generated using the TAO–CB complex (Fig. 1C). Both models suggest that ubiquinol is within ~4–5 Å of the diiron centre and the narrowness of the L-channel suggests that the ubiquinol tail will be in an extended conformation and will protrude from the cavity into the lipid bilayer by approximately six to seven isoprenoid units. We suggest that the bottleneck within the L-channel, although wide enough to accommodate the passage of ubiquinol (OH – OH — 6 Å), serves as a gate to position the substrate into the correct molecular orientation (Fig. 1C) to interact with the diiron centre such that the C2 – OH forms a hydrogen bond with R173 and S/T274 [15].

In an attempt to further probe this gating role of the highly conserved leucines within the L-channel, a number of mutant recombinant proteins were generated. Since all of the above residues are fully conserved in all species [1], mutant proteins were generated in the rSgAOX in order to compare the effects of such mutations with a well-documented mutation that affects both respiratory activity and the K_m for oxygen. In addition to the L177A and L267A mutants we also mutated R159 and D163 both of which are highly conserved across all species and located within the L-channel (Fig. 1B). Docking studies reveal that ubiquinol is able to bind with the aromatic head group occupying the same space as that of either colletochlorin B or AF2779OH within the active-site such that 1-OH interacts with R159 (see Fig. 1C and Ref. [16]). D163, which is equally very highly conserved, has also been previously suggested to be involved in ubiquinol-binding since in the presence of an inhibitor such as colletochlorin B, R173 forms a new hydrogen bond with D163, causing rotation in the position of R159 [1,15]. Given the assignment of R159 as a potential membrane binding residue, this implies that binding of the substrate within the active site causes a conformational change that would lower the effective binding to the membrane.

Table 1 summarises NADH dependent respiratory activity on membrane-bound SgAOX isolated from haem-A deficient cells expressed in *E. coli* strain FN102. Since this particular *E. coli* strain lacks glutamyl-tRNA reductase [31], it has a limited capacity to synthesise respiratory complexes *bd* and *bo*. Nevertheless both KCN and antimycin A were included in the assay medium to ensure that whatever limited respiratory complexes were still present their potential activity did not complicate respiratory measurements. Furthermore the lack of any effect of piericidin A or rotenone on NADH activity (data not shown) suggested that only NDH-2 was operative under these conditions and in agreement with our previous findings overall respiratory activity is not limited by substrate dehydrogenase but is fully controlled by AOX [36]. All of

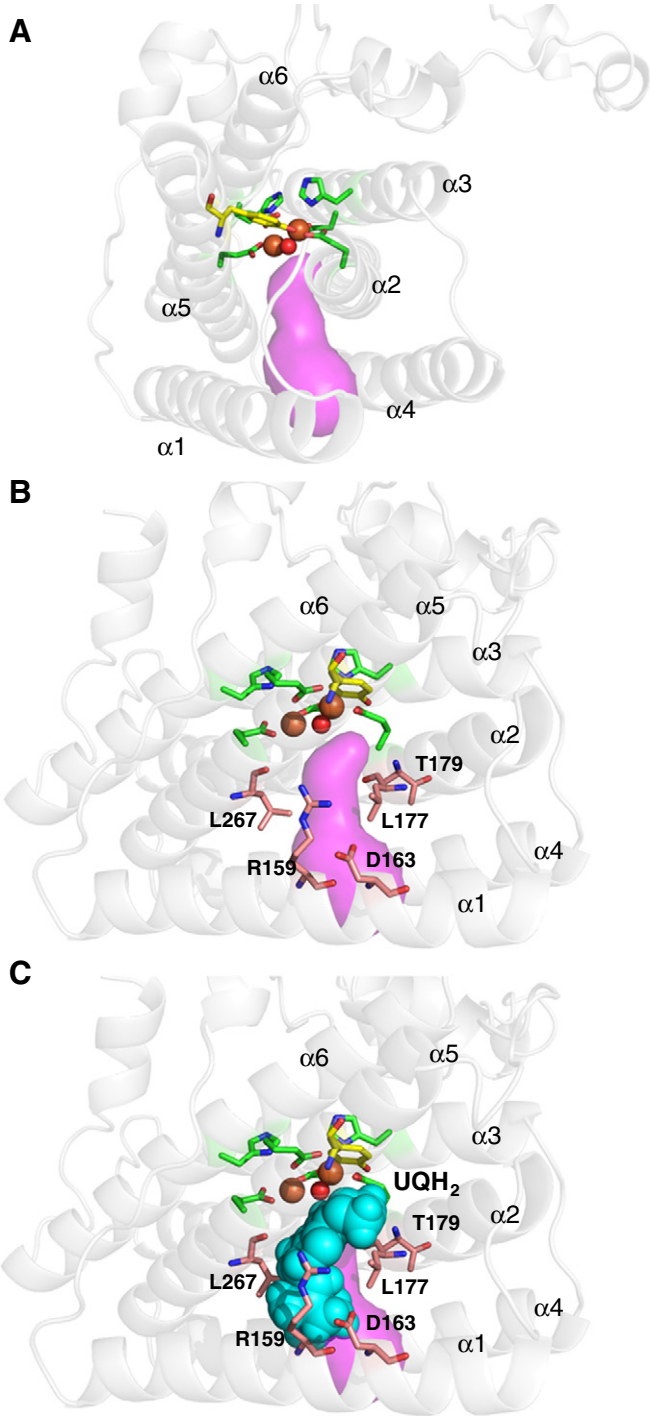

Fig. 1. Location of the ubiquinol-binding cavity in TAO. (A) A hydrophobic cavity (coloured purple) predicted for each monomer by CAVER protein-analysis software [39]. Helices are shown as grey cylinders and helices α1 and α4 anchor the protein to the inner membrane. Helices α2, α3, α5 and α6 act as a scaffold to bind the diiron centre. Brown spheres are diiron (Fe–OH^-–Fe) centre bridged by OH^- (red sphere), green sticks represent residues coordinating the diiron centre, and the yellow stick is the redox active Tyr275. (B) Location of the mutations (light pink sticks) examined in this study. (C) Location of ubiquinol binding predicted by the superposition of a ubiquinol molecule (cyan spheres) onto a bound inhibitor generated using PDB ID: 3W54. Oxygen and nitrogen atoms are coloured red and blue, respectively. Note the SgAOX numbering used throughout the figure. Figures were generated using PyMOL.

the mutants clearly exhibited respiratory rates that are lower than that of the wild-type. In SgAOX expressed in *E. coli* the T179A mutant also clearly had a major inhibitory impact upon respiratory activity comparable to that observed in *S. pombe* mitochondria [34]. The R159A (76% of control) and D163A (69%) mutations were equally as inhibitory whereas L177 or L267 mutations only inhibited the respiratory rate by approximately 50%. Addition of 10 mM pyruvate (data not shown) did not affect the respiratory activity of any of the mutants indicating that they are not regulated by α-keto acids, as is indeed the case for the wild-type *S. guttatum* AOX [34]. Fig. S1 indicates that although AOX is expressed in all mutants, total level of AOX expression is variable and does not appear to be related to activity when compared with Table 1. For instance, the L267A mutant appears to be expressed in similar quantities to wild-type but significantly more that the L177 mutant yet overall activity of both mutants is approximately 50% of control. Such results suggest that the mutation has a specific effect upon the activity of AOX and not merely an effect on the level of protein within the cell.

Table 1
Effect of site-specific mutations on the activity of membrane bound rSgAOX expressed in *E. coli* membranes.

Mutation	Specific activity (nmol O_2 min^{-1} mg^{-1})	Activity (%)	App K_m (O_2) (μM)
rSgAOX	230 ± 56	100%	13.1 ± 0.3
T179A	66 ± 36	28%	6.1 ± 0.4
D163A	72 ± 12	31%	5.9 ± 0.4
R159A	56 ± 19	24%	10.8 ± 0.2
L177A	118 ± 32	51%	8.9 ± 0.6
L267A	94 ± 3	41%	16.5 ± 1.2

Activities were measured using an oxygen electrode in 400 μl-50 mM Tris–HCl, pH 7.4, 10 mM pyruvate, 4 μM antimycin A and 1.25 mM NADH as the substrate, and apparent oxygen affinities [K_m (O_2)] were determined as described in Materials and methods. Data are averages ± S.E.M. of 2–5 separate membrane preparations. Percentage activity refers to percent of activity remaining relative to wild-type rSgAOX.

Fig. 2 shows typical O_2-dependencies of AOX activity. Fig. 2A indicates a respiratory trace obtained by wild-type AOX with NADH as a substrate and Fig. 2B is the derivative display. In the Eadie–Hofstee plots derived from these results we have only extracted data in the oxygen dependent region which as can be seen from Fig. 2C is linear. Such results are in agreement with similar measurements in rSgAOX expressed in *S. pombe* mitochondria [34] and strongly suggest that both wild-type and mutant AOX proteins exhibit simple Michaelis–Menten kinetics with respect to O_2. Average O_2 affinities calculated from 2 to 6 independent experiments are listed as apparent K_m (O_2) values in Table 1. The apparent K_m (O_2) of wild-type rSgAOX and the L267A mutant are approximately 14 μM which although slightly lower are nevertheless comparable to values determined with rSgAOX expressed in *S. pombe* [34] and importantly observed by others in plant mitochondria [40] suggesting that the expression system used in this study results in recombinant proteins that exhibit similar kinetic properties to that observed with isolated organelles. Importantly, the O_2 affinity of the T179A and D163A mutants is substantially higher than that of the wild-type enzyme. Less pronounced effects upon the apparent K_m (O_2) were also observed with the L177A and R159A mutants (Table 1) but these are probably not statistically significant when compared to wild-type. In all cases where a mutation resulted in an increase in oxygen affinity no change in the reaction stoichiometry of AOX could be detected (unpublished results) and remained consistent with a complete 4-electron reduction of O_2 to water.

In order to determine if any of these mutations have affected the interaction of AOX with its substrate, the sensitivity to a number of AOX antagonists were examined the inhibitory effects of which are summarised in Table 2. As in Table 1 1.25 mM NADH, in the presence of 4 μM antimycin A and 1 mM KCN, was used as the respiratory substrate and membranes were pre-incubated with inhibitor for approximately 2 min prior to addition of substrate. As is apparent from Table 1 both ascofuranone and colletochlorin B are far more potent inhibitors of SgAOX respiratory activity than conventional AOX inhibitors such as SHAM or octyl gallate. When the same inhibitors were tested on either the L177A or L267A mutant, however, IC_{50}s for all inhibitors increased substantially suggesting that such mutations conferred a high

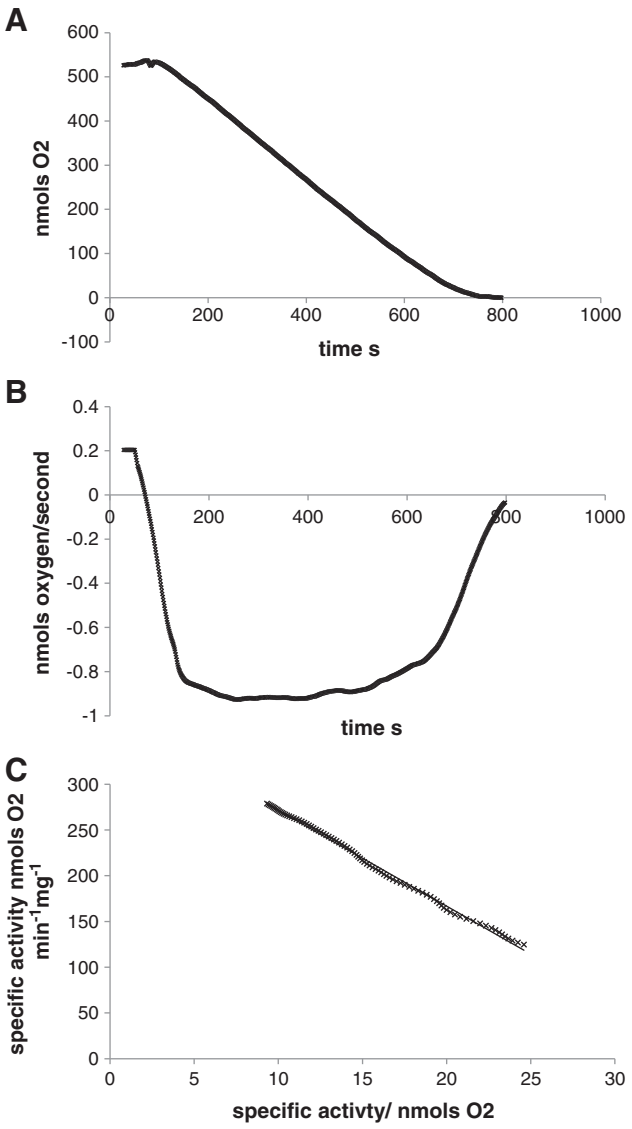

Fig. 2. O_2 affinities of wild-type and mutant rSgAOX expressed in *E. coli* membranes. (A) O_2 consumption was recorded continuously acquiring 40 data per minute; (for clarity, even distributions of only 50 data points are shown). (B) A typical derivative graph based upon the data obtained from the O_2 consumption measurements shown in A. Data were modelled assuming Michaelis–Menten kinetics to calculate O_2 affinities; typical experiments are shown, and averaged apparent K_m (O_2) values of 3–5 independent membrane preparations are given in Table 1. (C) Eadie–Hofstee representation of the respective data sets, fitted with linear expressions, confirming Michaelis–Menten behaviour with respect to O_2. Data at low O_2 (below 2.5 μM) were omitted as error in V/O_2 tends to infinity when O_2 approaches zero.

level of resistance compared to wild-type rSgAOX. In all cases, when the bottleneck within the hydrophobic cavity was removed IC_{50}s increased at least >20-fold (and in the case of ascofuranone >500-fold). In the case of SHAM no inhibition of the respiratory rate could be detected even at concentrations up to 500 μM. In an attempt to confirm whether or not changes in potency of the inhibitors were indeed a direct reflection of a widening of the channel we tested the effect of bulkier anti-malarial inhibitors, SL-2-25 and PG75 [41,42]. SL-2-25 and PG75 are diheteroaryl quinolones which are potent anti-malarial inhibitors. What is immediately obvious from Table 2 is that, when the bottleneck is removed by exchanging L177 and L267 for alanine, although the sensitivity to SL-2-25 remains unchanged, the sensitivity to PG75 increases approximately 10-fold particularly with the L267A mutant.

Table 2
Sensitivity of wild-type and mutant forms of rSgAOX expressed in *E. coli* membranes to AOX antagonists.

Inhibitor	wt IC_{50} μM	L177A IC_{50} μM	L267A IC_{50} μM
Colletochlorin B	0.45 ± 0.1	31 ± 2	35 ± 8
Ascofuranone	1.12 ± 0.2	>500	>500
Octylgallate	1 ± 0.4	>500	>500
SHAM	45 ± 8	N.I.	N.I.
SL-2-25	22 ± 10	4 ± 1	20 ± 5
PG75	5.3 ± 2	1.3 ± 0.01	0.48 ± 0.07

Oxygen consumption of wild-type and mutated forms of rSgAOX (approx. 1.25 mg/ml) expressed in *E. coli* membranes was measured as indicated in Materials and methods using 1.25 mM NADH as substrate. IC_{50} is the mid-point inhibition concentration and the values are the mean of 3 separate measurements. All data normalised by standardising the IC_{50} per rate (used 60 nmol O_2 min^{-1} mg^{-1}) and then correlated to the NADH rates given in Table 1 (51% — L177A, 41% — L267A). N.I. indicates that no inhibition was observed even at concentrations >500 μM.

4. Discussion

AOX within the blood-stream form of *T. brucei* and in phytopathogenic fungi is increasingly considered to be a valid drug and fungicide target as in all cases it appears essential for their continued life cycles [1] and with respect to trypanosomiasis the parasite is absent from the mammalian host [4]. Until recently little information on the nature of the AOX active-site was available rendering rational drug design, which targeted the AOX for the treatment of trypanosomiasis, difficult. Structural elucidation of the trypanosomal AOX, however, not only confirmed previous models that the enzyme is indeed a diiron protein but also demonstrated that under oxidised conditions it contains an unusual active-site geometry [15]. Importantly structural studies also revealed the nature of the inhibitor-binding site for both an ascofuranone derivative and colletochlorin B [15] is also revealed. In each case (both equally inhibit at sub-nM concentrations) the aromatic head is located close to the diiron active-site (within 4.3 Å of Fe2) and is held in position through a hydrogen bond network involving Y275 and E178 suggesting that the binding cavity for both is identical. We have previously demonstrated using CAVER protein-analysis software [1] (Fig. 1) that the diiron centre is connected to the bulk lipid phase of the membrane *via* a narrow hydrophobic cavity which is approximately 18–20 Å long [15,27]. A surprising structural feature of this cavity is that although the entrance is ~12 Å wide, a bottleneck formed by the presence of the L177 and L267 residues (~6 Å wide) can be detected 12–16 Å from the entrance to the cavity. Modelling studies reveal that ubiquinol binds in a similar manner to that of the AOX inhibitors described above namely with its head group within 4 Å of the diiron centre being held in position by a hydrogen bond network involving D163, R173, E178 and S/T274 [1,15]. Given the narrowness of the cavity such modelling studies suggest that the ubiquinol tail will be in an extended conformation with the end of the tail (6–7 isoprenoid units) protruding into the bulk lipid phase.

In this paper we have investigated the behaviour of several site-specific AOX mutants in a membrane environment where AOX is exposed to a natural substrate. The amino-acid residues we have identified, which are suggested to play important roles in substrate and/or inhibitor binding and are located within or close to the hydrophobic cavity [15], include R159, D163, L177 and L267 (Fig. 1). Structural analysis reveals that D163, located on helix α1 at the entrance to the cavity, is hydrogen bonded to R159 (helix α1) and R173 (helix α2) both of which we have previously suggested to be important for inhibitor and substrate-binding [1,15]. L177 and L267 are located on helices α2 and α5 respectively and, as is apparent from Fig. 1, form the bottleneck of the hydrophobic cavity.

We have previously demonstrated that mutation of the T179 residue to alanine in rSgAOX expressed in *S. pombe* mitochondria decreases both the apparent K_m (O_2) and maximum AOX activities [34]. The

results summarised in Table 1 are consistent with such effects, even when rSgAOX is expressed in *E. coli* membranes, suggesting that the mutational effects observed are indeed a reflection of an alteration in the enzyme's catalytic cycle and not due merely to alterations in membrane environment or cell type. This is a particularly important point since it not only validates the techniques used to measure such parameters but also means that justifiable comparisons can be made between AOXs expressed in different cell types. Indeed apparent K_m (O_2) for rSgAOX measured in this study is similar to that reported for mungbean (12.3 μM [43]) and soybean (13.2 μM [40,44]) mitochondria and equally comparable to that observed in the recombinant system expressed in *S. pombe* (20 μM [34]).

The data summarised in Table 1 suggests that those residues which are close to the diiron centre all result in a reduction in apparent K_m (O_2) when mutated. For instance the D163A, T179A and to a more limited extent L177A mutants all result in increased oxygen affinities whereas the R159 and L267 mutants remain statistically unchanged in comparison to wild-type enzyme. This at first may appear puzzling following an inspection of Fig. 1; however, it can perhaps be best explained by the location of these residues with respect to the position of the diirons, Fe 1 and Fe 2. Both L177 and T179 are located on helix α2 and flank E178, which co-ordinate with Fe1 [15], and both demonstrate an apparent K_m (O_2) which is lower than the wild-type value. We have previously suggested [34] that the influence of such mutations on AOX catalysis is probably indirect and due to subtle secondary-structure rearrangements that affect iron-ligating residues such as E178. The mutation of L267, however, had little effect upon the apparent K_m (O_2) even though it also flanks an iron-binding ligand (E268). In this case the iron-binding ligand is located on helix α5 and co-ordinates with Fe2 and not with Fe1 [1]. We have previously suggested that only Fe1 is involved in the initial stages of oxygen binding during the catalytic cycle [1,27] and hence any effect on the residues that ligate Fe1 is likely to have a deleterious effect on AOX catalysis.

Mutagenesis of D163 and R159 to alanine substantially decreases the maximum AOX activities to values comparable to each other and similar to that observed with T179. However in the case of D163 the apparent K_m (O_2) is reduced considerably whilst in the R159A mutant it remains the same as that of wild-type. As both of these residues are located on the same helix it is initially difficult to explain such a result particularly since examination of the crystal structure reveals that R159 is closer to the diiron core than D163 [15]. One explanation that could potentially accommodate such results is that should the D163A mutation result in destabilisation of the hydrogen bond formed between D163 and R173 then it may well result in a conformational change in helix α2. Such a result is not without precedent since we have previously demonstrated that a C172A mutation also leads to a reduction in the apparent K_m (O_2) [34] even though it is also some distance from the diiron core. This would suggest that the influence of both D163 and C172 on AOX catalysis is due to indirect secondary structure re-arrangements that affect the coordination of E178 to Fe1 and hence affect the turnover of the catalytic cycle [27].

Data summarised in Table 2 investigated the sensitivity of both wild-type and mutant forms of rSgAOX to various AOX antagonists in an attempt to determine if changes in the bottleneck of the hydrophobic cavity resulted in any change in inhibitor sensitivity. L177 and L267 appear to form the bottleneck (Fig. 1) and hence mutation to alanine removes the bulky isobutyl side chains thereby potentially widening the channel whilst still retaining its hydrophobic character. The results quite clearly demonstrated that mutation of either L177 or L267 decreased AOX sensitivity to all of the inhibitors tested. Importantly, however, it did dramatically increase the sensitivity to an anti-malarial compound (PG75) which we previously considered to be a poor AOX inhibitor (L. Young, A.L. Moore and G. Biagini, unpublished observations). SL-2-25 and PG75 are 2-diheteroaryl quinolones which in general are potent *Pf*NDH2 and cytochrome *Pf*bc1 Qo complex inhibitors [41,42]. In contrast to AOX inhibitors such as ascofuranone or colletochlorin B, they do not possess an isoprenoid tail but a 2-heteroaryl group and therefore lack the flexibility of the isoprenoid tail. An increase in sensitivity to PG75 following mutagenesis particularly of the L267 residue suggests that the mutations have indeed widened the hydrophobic cavity thereby providing access to the diiron centre by bulkier inhibitors such as PG75. We suggest that the location of these leucine residues at the entrance to the active-site helps to orientate both substrate and AOX antagonists into the correct conformation to interact with the diiron centre. Replacement with less bulky residues such as alanine removes this ability to correctly orientate the inhibitor and thereby, we would suggest, decreases sensitivity to AOX inhibitors. Importantly single amino acid mutations in inhibitor/substrate pockets have been found to be the cause of multi-drug resistant strains of malaria [41] and the decrease in sensitivity to main AOX antagonists, observed in the L-mutants studied in this report, suggests that an emergence of drug resistance to trypanosomiasis may also be possible. Therefore we suggest that the design of future AOX inhibitors should have structures that are less reliant on the orientation by the two-leucine residues.

In conclusion we have demonstrated in this paper that mutagenesis of a number of highly conserved residues (R159, D163, L177 and L267) to alanine, all of which line the hydrophobic inhibitor/substrate cavity in AOX, results in a decrease in maximum activity of AOX and in some cases (D163 and L177) a decrease in the apparent K_m (O_2). We have previously suggested that such an increase in apparent O_2 affinity implies a steady state rise of total AOX-bound oxygen [34]. This cannot result from an increase in initial O_2-association alone as we would not have observed inhibited enzyme turnover. Our data more likely suggest that the mutations observed in this report have altered the way in which the enzyme's catalytic cycle is controlled, and because maximum activity is decreased, they predict an increase in the steady state level of at least one O_2-derived AOX intermediate [27]. Such mutations should therefore prove to be useful in future stopped-flow and EPR experiments in our attempts to understand the mechanism of oxygen reduction and thereby facilitate the design of safer and more potent inhibitors for the treatment of diseases in which the AOX plays a pivotal role such as for instance in trypanosomiasis.

Supplementary data to this article can be found online at http://dx.doi.org/10.1016/j.bbabio.2014.01.027.

Acknowledgements

The authors are grateful to Dr. Giancarlo Biagini (Liverpool School of Tropical Medicine, University of Liverpool, UK) for the kind gift of SL-2-25 and PG75. This work was supported in part by the Creative Scientific Research Grant 18GS0314 (to K.K.), Grant-in-aid for Scientific Research on Priority Areas 18073004 (to K.K.) from the Japanese Society for the Promotion of Science (JSPS), Targeted Proteins Research Program (to K.K. and S.H.) from the Japanese Ministry of Education, Science, Culture, Sports and Technology (MEXT), Grant-in-aid for research on emerging and re-emerging infectious diseases from the Japanese Ministry of Health and Welfare (to K.K.), and the Programme for Promotion of Basic and Applied Researches for Innovations in Bio-oriented Industry (BRAIN) (to K.K. and S.H.). A.L.M. gratefully acknowledges BBSRC and the University of Sussex for financial support, with K.K. the Prime Ministers Initiative 2 (Connect — British Council) fund for collaborative twinning and JSPS for a Travel Fellowship. L.Y. and B.S. gratefully acknowledge the University of Sussex and JS the BBSRC (CASE Award) for studentship support.

References

[1] A.L. Moore, T. Shiba, L. Young, S. Harada, K. Kita, K. Ito, Unraveling the heater: new insights into the structure of the alternative oxidase, Annu. Rev. Plant Biol. 64 (2013) 637–663.

[2] A.E. McDonald, G.C. Vanlerberghe, Origins, evolutionary history, and taxonomic distribution of alternative oxidase and plastoquinol terminal oxidase, Comp. Biochem. Physiol. D 1 (2006) 357–364.

[3] M. Chaudhuri, W. Ajayi, G.C. Hill, Biochemical and molecular properties of the *Trypanosoma brucei* alternative oxidase, Mol. Biochem. Parasitol. 95 (1998) 53–68.
[4] M. Chaudhuri, R.D. Ott, G.C. Hill, Trypanosome alternative oxidase: from molecule to function, Trends Parasitol. 22 (2006) 484–491.
[5] C.W. Roberts, F. Roberts, F.L. Henriquez, D. Akiyoshi, B.U. Samuel, T.A. Richards, W. Milhous, D. Kyle, L. McIntosh, G.C. Hill, M. Chaudhuri, S. Tzipori, R. McLeod, Evidence for mitochondrial-derived alternative oxidase in the apicomplexan parasite *Cryptosporidium parvum*: a potential anti-microbial agent target, Int. J. Parasitol. 34 (2004) 297–308.
[6] T. Suzuki, T. Hashimoto, Y. Yabu, Y. Kido, K. Sakamoto, C. Nihei, M. Hato, S. Suzuki, Y. Amano, K. Nagai, T. Hosokawa, N. Minagawa, N. Ohta, K. Kita, Direct evidence for cyanide-insensitive quinol oxidase (alternative oxidase) in apicomplexan parasite *Cryptosporidium parvum*: phylogenetic and therapeutic implications, Biochem. Biophys. Res. Commun. 313 (2004) 1044–1052.
[7] D.M. Standley, M. van der Giezen, Modeling the alternative oxidase from the human pathogen *Blastocystis* using automated hybrid structural template assembly, Res. Rep. Biochem. 2 (2012) 1–8.
[8] L. Yan, M. Li, Y. Cao, P. Gao, Y. Cao, Y. Wang, Y. Jiang, The alternative oxidase of *Candida albicans* causes reduced fluconazole susceptibility, J. Antimicrob. Chemother. 64 (2009) 764–773.
[9] G.A.M. Cross, Fat-free proteins kill parasites, Nature 464 (2010) 689–690.
[10] C. Nihei, Y. Fukai, K. Kita, Trypanosome alternative oxidase as a target of chemotherapy, Biochim. Biophys. Acta 1587 (2002) 234–239.
[11] K. Kita, C. Nihei, E. Tomitsuka, Parasite mitochondria as drug target: diversity and dynamic changes during the life cycle, Curr. Med. Chem. 10 (2003) 2535–2548.
[12] K. Nakamura, S. Fujioka, S. Fukumoto, N. Inoue, K. Sakamoto, H. Hirata, Y. Kido, Y. Yabu, T. Suzuki, Y. Watanabe, H. Saimoto, H. Akiyama, K. Kita, Trypanosome alternative oxidase, a potential therapeutic target for sleeping sickness, is conserved among *Trypanosoma brucei* subspecies, Parasitol. Int. 59 (2010) 560–564.
[13] Y. Yabu, A. Yoshida, T. Suzuki, C. Nihei, K. Kawai, N. Minagawa, T. Hosokawa, K. Nagai, K. Kita, N. Ohta, The efficacy of ascofuranone in a consecutive treatment on *Trypanosoma brucei brucei* in mice, Parasitol. Int. 52 (2003) 155–164.
[14] Y. Yabu, T. Suzuki, C. Nihei, N. Minagawa, T. Hosokawa, K. Nagai, K. Kita, N. Ohta, Chemotherapeutic efficacy of ascofuranone in *Trypanosoma vivax*-infected mice without glycerol, Parasitol. Int. 55 (2006) 39–43.
[15] T. Shiba, Y. Kido, D.K. Inaoka, E.O. Balogun, K. Sakamoto, T. Nara, T. Aoki, T. Honma, A. Tanaka, M.S. Inoue, S. Matsuoka, A.L. Moore, S. Harada, K. Kita, The structure of the trypanosomal cyanide-insensitive alternative oxidase, Proc. Natl. Acad. Sci. U. S. A. 110 (2013) 4580–4585.
[16] M.E. Andersson, P. Nordlund, A revised model of the active site of alternative oxidase, FEBS Lett. 449 (1999) 17–22.
[17] D. Berthold, M.E. Andersson, P. Nordlund, New insight into the structure and function of the alternative oxidase, Biochim. Biophys. Acta 1460 (2000) 241–254.
[18] M.S. Albury, C. Affourtit, A.L. Moore, A highly conserved glutamate residue (E270) is essential for alternative oxidase activity, J. Biol. Chem. 273 (1998) 30301–30305.
[19] M. Chaudhuri, W. Ajayi, G.C. Hill, Biochemical and molecular properties of the *Trypanosoma brucei* alternative oxidase, Mol. Biochem. Parasitol. 95 (1998) 53–68.
[20] W.U. Ajayi, M. Chaudhuri, G.C. Hill, Site-directed mutagenesis reveals the essentiality of the conserved residues in the putative diiron active site of the trypanosome alternative oxidase, J. Biol. Chem. 277 (2002) 8187–8193.
[21] M.S. Albury, C. Affourtit, P.G. Crichton, A.L. Moore, Structure of the plant alternative oxidase — site-directed mutagenesis provides new information on the active site and membrane topology, J. Biol. Chem. 277 (2002) 1190–1194.
[22] K. Nakamura, K. Sakamoto, Y. Kido, Y. Fujimoto, T. Suzuki, M. Suzuki, Y. Yabu, N. Ohta, A. Tsuda, M. Onuma, K. Kita, Mutational analysis of the *Trypanosoma vivax* alternative oxidase: the $E(X)_6Y$ motif is conserved in both mitochondrial alternative oxidase and plastid terminal oxidase and is indispensable for enzyme activity, Biochem. Biophys. Res. Commun. 334 (2005) 593–600.
[23] D.A. Berthold, N. Voevodskaya, P. Stenmark, A. Gräslund, P. Nordlund, EPR studies of the mitochondrial alternative oxidase — evidence for a diiron carboxylate center, J. Biol. Chem. 277 (2002) 43608–43614.
[24] A.L. Moore, J.E. Carré, C. Affourtit, M.S. Albury, P.G. Crichton, K. Kita, P. Heathcote, Compelling EPR evidence that the alternative oxidase is a diiron carboxylate protein, Biochim. Biophys. Acta 1777 (2008) 327–330.
[25] A. Maréchal, Y. Kido, K. Kita, A.L. Moore, P.R. Rich, Three redox states of *Trypanosoma brucei* alternative oxidase identified by infrared spectroscopy and electrochemistry, J. Biol. Chem. 284 (2009) 31827–31833.
[26] D.A. Berthold, P. Stenmark, Membrane-bound di-iron carboxylate proteins, Annu. Rev. Plant Biol. 54 (2003) 497–517.
[27] L. Young, T. Shiba, S. Harada, K. Kita, M.S. Albury, A.L. Moore, The alternative oxidases: simple oxidoreductase proteins with complex functions, Biochem. Soc. Trans. 41 (2013) 1305–1311.
[28] M. Iwata, Y. Lee, T. Yamashita, T. Yagi, S. Iwata, A.D. Cameron, M.J. Maher, The structure of the yeast NADH dehydrogenase (Ndi1) reveals overlapping binding sites for water- and lipid-soluble substrates, Proc. Natl. Acad. Sci. U. S. A. 109 (2012) 15247–15252.
[29] D. Picot, P.J. Loll, R.M. Garavito, The X-ray crystal structure of the membrane protein prostaglandin H_2 synthase-1, Nature 367 (1994) 243–249.
[30] R. Baradaran, J.M. Berrisford, G.S. Minhas, L.A. Sazanov, Crystal structure of the entire respiratory complex I, Nature 494 (2013) 443–450.
[31] C. Nihei, Y. Fukai, K. Kawai, A. Osanai, Y. Yabu, T. Suzuki, N. Ohta, N. Minagawa, K. Nagai, K. Kita, Purification of active recombinant trypanosome alternative oxidase, FEBS Lett. 538 (2003) 35–40.
[32] M.G. Claros, P. Vincens, Computational method to predict mitochondrially imported proteins and their targeting sequences, Eur. J. Biochem. 241 (1996) 779–786.
[33] D.M. Rhoads, L. McIntosh, Isolation and characterization of a cDNA clone encoding an alternative oxidase protein of *Sauromatum guttatum* (Schott), Proc. Natl. Acad. Sci. U. S. A. 88 (1991) 2122–2126.
[34] P.G. Crichton, M.S. Albury, C. Affourtit, A.L. Moore, Mutagenesis of the plant alternative oxidase reveals features important features for oxygen binding and catalysis, Biochim. Biophys. Acta 1797 (2010) 732–737.
[35] K. Maundrell, nmt1 of fission yeast — a highly transcribed gene completely repressed by thiamine, J. Biol. Chem. 265 (1990) 10857–10864.
[36] C. Affourtit, K. Krab, A.L. Moore, Control of plant mitochondrial respiration, Biochim. Biophys. Acta 1504 (2001) 59–70.
[37] K.M. Chen, M.M. Joullie, Synthesis of colletochlorin-D, Tetrahedron Lett. 23 (44) (1982) 4567–4568.
[38] J. Sambrook, E.F. Fritsch, T. Maniatis, Molecular Cloning: A Laboratory Manual, Cold Spring Harbor Laboratory, Cold Spring Harbor, NY, 1989.
[39] P. Medek, P. Benes, J. Sochor, Computation of tunnels in protein molecules using Delaunay triangulation, J. WSCG 15 (2007) 107–114.
[40] M. Ribas-Carbo, J.A. Berry, J. Azcon-Bieto, J.N. Siedow, The reaction of the plant mitochondrial cyanide-resistant alternative oxidase with oxygen, Biochim. Biophys. Acta 1188 (1994) 205–212.
[41] G.A. Biagini, N.E. Fisher, A.E. Shone, C. Pidathala, M.A. Mubarakia, A. Srivastava, A. Hill, T. Antoine, A.J. Warman, J. Davies, C. Pidathala, R.K. Amewu, S.C. Leung, R. Sharma, P. Gibbons, D.W. Hong, B. Pacorel, A.S. Lawrenson, S. Charoensutthivarakul, L. Taylor, O. Berger, A. Mbekeani, P.A. Stocks, G.L. Nixon, J. Chadwick, J. Hemingway, M.J. Delves, R.E. Sinden, A.-M. Zeeman, C.H.M. Kocken, N.G. Berry, P.M. O'Neill, S.A. Ward, Generation of quinolone antimalarials targeting the *Plasmodium falciparum* mitochondrial respiratory chain for the treatment and prophylaxis of malaria, Proc. Natl. Acad. Sci. (USA) 109 (2012) 8298–8303.
[42] C. Pidathala, R. Amewu, B. Pacorel, G.L. Nixon, P. Gibbons, W.D. Hong, S.C. Leung, N.G. Berry, R. Sharma, P.A. Stocks, A. Srivastava, A.E. Shone, S. Charoensutthivarakul, L. Taylor, O. Berger, A. Mbekeani, A. Hill, N.E. Fisher, A.J. Warman, G.A. Biagini, S.A. Ward, P.M. O'Neill, Identification, design and biological evaluation of bisaryl quinolones targeting *Plasmodium falciparum* type II NADH:quinone oxidoreductase (PfNDH2), J. Med. Chem. 55 (5) (2012) 1831–1843.
[43] K.J. Gupta, A. Zabalza, J.T. van Dongen, Regulation of respiration when the oxygen availability changes, Physiol. Plant. 137 (2009) 383–391.
[44] A.H. Millar, F.J. Bergersen, D.A. Day, Oxygen-affinity of terminal oxidases in soybean mitochondria, Plant Physiol. Biochem. 32 (1994) 847–852.